Global NEST Journal, Vol 16, No 3, pp 445-454, 2014

MODELLING MICROPOLLUTANT REMOVAL BY SOLAR PHOTO-FENTON

CARRA I.[1,2]
GARCÍA SÁNCHEZ J.L.[1,2]
MALATO S.[2,3]
SÁNCHEZ PÉREZ J.A. [1,2,*]

[1]*Department of Chemical Engineering*
University of Almería
04120 Almería, Spain
[2]*CIESOL, Joint Centre of the University of Almería-CIEMAT*
04120 Almería, Spain
[3]*Plataforma Solar de Almería (CIEMAT),*
04200 Tabernas (Almería), Spain

Received: 27/12/13
Accepted: 11/02/14
Available online: 12/02/2014

*to whom all correspondence should be addressed
e-mail: jsanchez@ual.es

ABSTRACT

This paper is focused on modelling the degradation of micropollutants by solar photo-Fenton at pilot plan scale. To this aim, a three pesticide mixture (acetamiprid, thiabendazole and imazalil, 100 µg l^{-1} each) was treated by photo-Fenton in simulated secondary effluent. The model covered a wide interval of catalyst concentration (1 to 20 mg l^{-1} Fe) and solar irradiance (5 to 30 W m^{-2}). A Monte Carlo direct search was used to determine the kinetic constants which adjusted pesticide removal and hydrogen peroxide consumption in the selected experimental conditions (identification runs). The model was validated with experimental conditions different from the identification step (validation runs). Hydrogen peroxide consumption and pollutant degradation could be predicted adequately for all irradiances and iron concentrations higher than 5 mg l^{-1} Fe. As a result, the presented model could predict the treatment time during the whole year, as it is valid for a wide range of irradiation and for commonly used values of catalyst concentration.

Keywords: acetamiprid, thiabendazole, imazalil, simulation, photocatalysis, iron, hydrogen peroxide

1. Introduction

The use of advanced oxidation processes (AOPs) to remove organic pollutants has spread over the last decades (Karcin *et al.*, 2013, Michael *et al.*, 2013). The development in new analytical techniques in recent years has also allowed detecting pollutants in very low concentrations (up to ng l^{-1}) (Hisaindee *et al.*, 2013), for which they are called "micropollutants". Their low concentration seldom results in high toxicity, but they are persistent and can accumulate in water surfaces such as rivers or lakes (Al Aukidy *et al.*, 2012; Bueno *et al.*, 2013). Different AOPs have been used to address this problem, being the photo-Fenton process one of the most successful alternatives (Ikehata *et al.*, 2006). This process oxidises the organic matter mainly with hydroxyl radicals, although other less-reactive radicals can be implicated as well. The radicals are generated by a series of chain reactions initiated by the combination of Fe (II) (catalyst) and hydrogen peroxide (reactant) and where irradiance in the UV-Vis spectrum plays an important role, enhancing the process rate.

The source of irradiance can be the solar light, thus operating costs decrease. However, this technology has not spread at a commercial scale yet, even though the feasibility of the process is not questioned (Blanco *et al.*, 2013; Malato *et al.*, 2009, Sánchez Pérez *et al.*, 2013a). One of the keys to introduce this technology at commercial scale is the automatisation of the operation. Before this step is taken, we

must be able to predict the outcome of the process (treatment time and reactant degradation) as well as the operating conditions. This is especially difficult for a solar-driven process, where irradiance is an environmental variable which cannot be controlled. Some attempts have been tried at higher pollutant concentrations (Cabrera Reina *et al.*, 2012; Kusic *et al.*, 2009; Li Puma *et al.*, 2004), but as far as the authors know, not for micropollutants.

The aim of this work is to obtain a reliable and simplified kinetic model which can predict the degradation at pilot plant scale of a micropollutant mixture formed by acetamiprid (ACTM), thiabendazole (TBZ) and imazalil (IMZ) with solar photo-Fenton in a wide interval of iron concentration (1 - 20 mg l^{-1}) and solar UV irradiance (5 - 30 W m^{-2}). The model is focused on predicting micropollutant degradation and hydrogen peroxide consumption profiles in simulated secondary wastewater.

2. Methods

2.1 Reagents

High purity ACTM, TBZ and IMZ were supplied by Sigma–Aldrich. Sulphuric acid (95–97%) and hydrogen peroxide (35%) were obtained from J.T. Baker and ferrous sulphate (99%) from Fluka. $CaSO_4 \cdot 2H_2O$, $MgSO_4$, KCl, $(NH_4)_2SO_4$, K_2HPO_4, $NaHCO_3$, beef extract, peptone, humic salts, tannic acid, sodium lignin sulfonate, sodium lauryle sulphate, acacia gum powder, and arabic acid were acquired from Sigma-Aldrich. HPLC grade acetonitrile from Carlo Erba Reagents and Milli-Q grade water were used as the mobile phase in the chromatographic analysis.

2.2 Experimental set-up

The constituents of the simulated secondary effluent from a municipal wastewater treatment plant were $CaSO_4 \cdot 2H_2O$ (60 mg l^{-1}), $MgSO_4$ (60 mg l^{-1}), KCl (4 mg l^{-1}), $(NH_4)_2SO_4$ (23.6 mg l^{-1}), K_2HPO_4 (7.0 mg l^{-1}), $NaHCO_3$ (96 mg l^{-1}), beef extract (1.8 mg l^{-1}), peptone (2.7 mg l^{-1}), humic salts (4.2 mg l^{-1}), tannic acid (4.2 mg l^{-1}), sodium lignin sulfonate (2.4 mg l^{-1}), sodium lauryle sulphate (0.9 mg l^{-1}), acacia gum powder (4.7 mg l^{-1}), and arabic acid (5.0 mg l^{-1}) (Zhang *et al.*, 2007). The dissolved organic carbon, DOC, was over 17 mg l^{-1}. The optical properties of the simulated effluent in the range of UV-A/Vis are the same as in demineralised water.

Solar photo-Fenton experiments were carried out in an outdoor pilot plant. It is a tubular reactor with four independent loops which permit to run simultaneous experiments under the same incident solar light (Figure 1). The tubes are made of borosilicate glass. In each experiment, 7 l were treated (4.55 l irradiated volume). The pilot plant is located at the Centro de Investigación de la Energía Solar (CIESOL), in Almería, Spain (latitude 36° 50' 24.59" N, longitude 2° 28' 4.52" W). The photoreactor has a path length of 5 cm (tube diameter). UVA radiation is measured using a global UV radiometer (DeltaOhm, LP UVA 02 AV; spectral response 327-384 nm) mounted on a platform tilted at 37°, matching the local latitude and providing data in terms of incident UV (W m^{-2}).

Also, the plant is equipped with pH and temperature probes and the variables were monitored on-line by means of a LabJack USB/Ethernet data acquisition device connected to a computer. At the beginning of the experiment, the tubular reactor was covered. A turbulent recirculation time of 5 minutes was allowed for homogenisation after the addition of each reagent, corresponding to the mixing time in the photoreactor. After this time, the solar collector was uncovered and photo-Fenton reaction began. The pH was adjusted to 2.8. In all cases, 50 mg l^{-1} H_2O_2 was used. Values for Fe concentration were: 1, 5 and 20 mg l^{-1} Fe. Regarding UV incident radiation, different values were able to be obtained outdoors through the use of meshes which partially filtered solar irradiance: 5, 15, 20 and 30 W m^{-2} of UVA was able to be achieved (with a temperature of 25±2 °C. The process was run at noon, when irradiance was virtually constant for the duration of the tests. The operating conditions are summarised in Table 1.

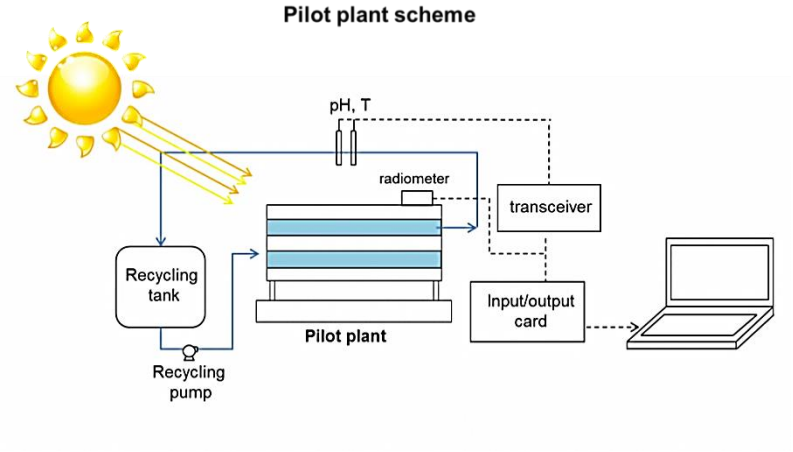

Figure 1. Process scheme in the tubular pilot plant

Table 1. Experimental conditions for identification and validation runs

Run	[Fe] (mg l^{-1})	Irradiance (W m^{-2})	Use
1	1	5	Identification
2	1	15	Identification
3	1	20	Validation
4	1	30	Identification
5	5	5	Validation
6	5	15	Identification
7	5	20	Identification
8	5	30	Identification
9	20	5	Identification
10	20	15	Validation
11	20	20	Identification
12	20	30	Identification

2.3 Chemical analysis

The sample volume was 10 ml. All samples were immediately filtered (0.20 µm-diameter nylon filters from Millipore®) and the filter was washed with acetonitrile in a relationship acetonitrile:sample 1:10 and mixed with the filtered water sample. This is because acetonitrile acts as an $HO^{\bullet}$ scavenger, stopping the reaction (Mitroka *et al.*, 2010) and also sweeps out any trace of pollutant that may have been retained by the filter. This served to prevent any possible adsorption on iron precipitate or in the filter.

Hydrogen peroxide was measured by a colorimetric method using ammonium metavanadate, recording the absorbance value at 450 nm (Nogueira *et al.*, 2005). The concentration of iron was determined according to the o-phenantroline standardized procedure (ISO 6332) and the red complex formed was determined spectrophotometrically at 510 nm.

ACTM, TBZ and IMZ concentrations were determined by means of liquid chromatography (UPLC Agilent 1200 Series equipped with a column oven, degasser, autosampler and diode array detector) with a reversed-phase column (Agilent XDB-C18). The mobile phase consisted of a gradient mixture of acetonitrile and 1% v/v formic acid in water. It was a 15 min method. The gradient started at 5% acetonitrile, increasing to 15% after 7 min, to 50% after 12min and reaching 100% at the end of the method. Retention times were 4.4 for TBZ, 9.6 for ACTM and 11.4 for IMZ. The detection wavelengths were 225 nm for IMZ, 248 nm for ACTM and 300 nm for TBZ. The gradient used was initially set at 5%

acetonitrile, progressively increasing the concentration to 100% over a 15 min run. The limit of detection (LOD) was 2 μg l^{-1} for ACTM, 1 μg l^{-1} for TBZ and 10 μg l^{-1} for IMZ.

2.4 Modelling

The model was based on a simplification of the reactions that take place in the photo-Fenton process and which are represented in Table 2. The reactions can be classified in three types: the iron redox cycle reactions (Eqs. 1-3); the oxidation of pollutant and other organic molecules (OM) (Eqs. 4-7); and reactions of hydroxyl radicals with themselves and with hydrogen peroxide, which are considered inefficient as the radicals are not used to oxidise the pollutants (Eqs. 8-9) (Gogate *et al.*, 2004). The model assumes eight species: Fe^{2+}, Fe^{3+}, hydrogen peroxide, ACTM, TBZ, IMZ, OM, and both hydroxyl and perhydroxyl radicals, which are named R in the model as both oxidise the organic compounds and the probability of reaction with them is the same. The target was to degrade micropollutants not their mineralization or the mineralization of other organics. Therefore, oxidation till carbon dioxide release was not considered in this model.

Table 2. Reaction scheme in the photo-Fenton process

Iron redox cycle reactions	
$Fe^{2+} + H_2O_2 \rightarrow Fe^{3+} + HO^{\bullet} + HO^-$	(1)
$Fe^{3+} + H_2O + h\nu \rightarrow Fe^{2+} + HO^{\bullet} + H^+$	(2)
$Fe^{3+} + H_2O_2 \rightarrow Fe^{2+} + HOO^{\bullet} + H^+$	(3)
Parent compound and organic matter oxidation	
$HO^{\bullet}$ + ACTM → ACTM*	(4)
$HO^{\bullet}$ + TBZ → TBZ *	(5)
$HO^{\bullet}$ + IMZ → IMZ*	(6)
$HO^{\bullet}$ + OM → OM*	(7)
Inefficient reactions	
$H_2O_2 + HO^{\bullet} \rightarrow H_2O$	(8)
$HO^{\bullet} + HO^{\bullet} \rightarrow H_2O + ½\ O_2$	(9)

The reaction rates and mass balances proposed for the system are shown in Tables 3 and 4. Note that solar UV irradiance was considered as another variable in the kinetics and was denoted as I (Eq. 12). This was necessary as the photo-Fenton process depends on the irradiance that reaches the reactor's surface.

Table 3. Kinetic expressions for each reaction

Kinetic rates	
$r_1=k_1\cdot[Fe^{2+}]\cdot[H_2O_2]$	(11)
$r_2=k_2\cdot[Fe^{3+}]\cdot I/(k_{2s}+I)$	(12)
$r_3=k_3\cdot[\ Fe^{3+}]\cdot[H_2O_2]$	(13)
$r_4=k_4\cdot[R]\cdot[ACTM]$	(14)
$r_5=k_5\cdot[R]\cdot[TBZ]$	(15)
$r_6=k_6\cdot[R]\cdot[IMZ]$	(16)
$r_7=k_7\cdot[R]\cdot[H_2O_2]$	(17)
$r_8=k_8\cdot[R]^2$	(18)
$r_9=k_9\cdot[R]\cdot[OM]$	(19)

In addition, the fraction of illuminated volume in the system was taken into account in the mass balances (ratio V_i/V_t =0.65) (Table 4).

Table 4. Mass balances on the system

$\frac{d[Fe^{2+}]}{dt} = -r_1 + \frac{V_i}{V_t} \cdot r_2 + \left(1 - \frac{V_i}{V_t}\right) \cdot r_3$	(20)
$\frac{d[Fe^{3+}]}{dt} = r_1 - \frac{V_i}{V_t} \cdot r_2 - \left(1 - \frac{V_i}{V_t}\right) \cdot r_3$	(21)
$\frac{d[H_2O_2]}{dt} = -r_1 - \left(1 - \frac{V_i}{V_t}\right) \cdot r_3 - r_8$	(22)
$\frac{d[R]}{dt} = r_1 + \frac{V_i}{V_t} \cdot r_2 + \left(1 - \frac{V_i}{V_t}\right) \cdot r_3 - r_4 - r_5 - r_6 - r_7 - r_8 - r_9$	(22)
$\frac{d[ACTM]}{dt} = -r_4$	(22)
$\frac{d[TBZ]}{dt} = -r_5$	(22)
$\frac{d[IMZ]}{dt} = -r_6$	(23)
$\frac{d[OM]}{dt} = -r_9$	(24)

The aim of the model was to predict the time course variation in the main four process variables: ACTM, TBZ, IMZ and H_2O_2 concentrations. For this purpose, 10 parameters in the model had to be obtained. They were the kinetic constants k_1, k_2, k_{2s}, k_3, k_4, k_5, k_6, k_7, k_8, k_9. The kinetic rates and mass balances were implemented in MATLAB® to find the best values for the 10 parameters to model the four aforementioned variables. The modelling was executed implementing a Monte Carlo direct search with an error rate as objective function in a sequential search. Thus, the method searched randomly values for the parameters in a wide interval in the order of magnitude found in literature for each constant. Then, the values were used to model the variables profiles in the experimental conditions of the identification runs (Table 1). The simulated profiles were then compared to the experimental data. The comparison was made by the error rate objective function:

$$E = \sum_{n=1}^{4} e_n \tag{25}$$

where *E* is the sum of the errors for each variable, subscript *n* stands for the modelled variable (ACTM, TBZ, IMZ and hydrogen peroxide); and e_n is the error of each variable and calculated through Eq. 26. This strategy has been used in previous work (Cabrera Reina *et al.*, 2012).

$$e_n = \alpha_n \cdot \sum_{i=1}^{9} \sum_{t=0}^{t=t_f} \left[\frac{x_{sim,t} - x_{exp,t}}{x_{exp,t}} \right]^2 \tag{26}$$

The subscript *i* stands for each identification run; *t* is the time when the variable was measured; *sim* stands for the simulated value; and *exp,* for the measured value; α is a weighting parameter to define the contribution and importance of each parameter to the model. The value of alpha was 4, 2, 1 and 3 for ACTM, TBZ, IMZ and hydrogen peroxide, respectively. Model validation was performed by comparing predicted and experimental data for the validation runs (Table 1). These runs were taken as representative of the assayed operating conditions.

3. Results and discussion

Solar photo-Fenton was carried out at pilot plant scale in simulated secondary effluent with slight hydrogen peroxide excess (50 mg l^{-1}) to avoid radical limitation. Iron concentration was varied from 1 to

20 mg l^{-1} as they are common amounts used for this kind of application (De la Cruz *et al.*, 2012; Klamerth *et al.*, 2013; Malato *et al.*, 2004); and the achieved irradiance ranged from 5 to 30 W m^{-2}, which covers from winter to summer conditions and sunrise to sunset. The validation of the model in such wide intervals of catalyst and irradiation conditions is important for the automatisation of the process. The three model pollutants have been found in wastewater treatment plant effluents with concentrations between 50-100 ng l^{-1} (Bernabeu *et al.*, 2011; Ortelli *et al.*, 2005). Nevertheless, a concentration of 100 µg l^{-1} was used, which was low enough to be considered a micropollutant mixture, but high enough to monitor through UPLC.

To illustrate the effect of UV irradiance on the removal of ACTM, TBZ and IMZ as well as on H_2O_2 consumption, the profiles obtained with 5 mg l^{-1} Fe are shown in Figure 2. The effect of UV irradiance at this concentration was representative of 1 and 20 mg l^{-1} Fe. Although the global process rate increased or decreased with increasing/decreasing amounts of iron, the effects observed were the same for every iron concentration.

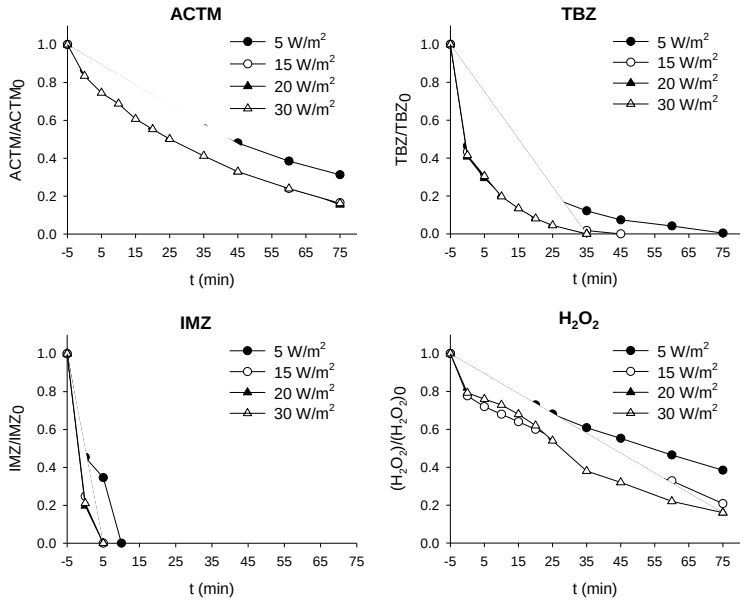

Figure 2. Experimental results obtained for 5 mg l^{-1} Fe and all irradiances assayed

Among the three micropollutants, ACTM was the less reactive and thus, the slowest to be oxidised, followed by TBZ and IMZ. This fact made ACTM the target pollutant, since ensuring it was removed would imply the other two would be as well. It could also be observed that the increase in solar UV irradiance from 5 to 15 W m^{-2} resulted in an increase in the degradation rate, but the increase in irradiance above that value did not improve the degradation rate. The same could also be observed for hydrogen peroxide consumption. This effect occurred for the other two iron concentrations as well.

This can be explained considering that above certain UV irradiance (15 W m^{-2} in this case) enough radicals were generated to oxidise the parent compounds, which were in very low concentrations. Consequently, a rise in solar UV irradiance above that value resulted in a situation of radical excess where no improvement could be achieved in the kinetic rate. This fact was taken into account when the model was designed. The generation of an excess of radicals implies there was irradiance saturation (excess) as well. Thus, the kinetic corresponding to reaction 2, which is where irradiance is directly involved in the process, had to include it. Indeed, in the kinetic rate expression (Eq. 12) the term $(I+k_{s2})$ was incorporated in the denominator to consider the saturation effect of irradiance, where k_{2s} is the saturation constant. The values obtained for model parameters are presented in Table 5.

The highest kinetic constants corresponded to k_4-k_6 and k_8. The value of k_8 is related to the radical-radical inefficient reaction (Eq. 18), which in this case involves hydroxyl and perhydroxyl radicals. This

agrees with the literature, where the kinetics between the radicals is very fast (Kusic *et al.*, 2006; Ortiz de la Plata *et al.*, 2010). As for the oxidation of ACTM, TBZ and IMZ, the corresponding constants met the condition $k_4<k_5<k_6$, as ACTM was the slowest to be oxidized, then TBZ and then IMZ. Certainly, IMZ's kinetic constant was over 10 times higher than ACTM's.

Table 5. Model parameters in $mM^{-1}\ s^{-1}$

k_1	k_2[a]	k_{2s}[b]	k_3	k_4	k_5	k_6	k_7	k_8	k_9
350	3	7	0.05	1012	5053	12350	140	10276	34

[a] k_2 is expressed in h^{-1}

[b] k_{2s} is expressed in $W\ m^{-2}$

The value of k_9, related to the oxidation of other organic molecules, was rather low (34 $mM^{-1}\ s^{-1}$). This is reasonable since usually other organic molecules present in a secondary effluent have a high oxidation state, so their reactivity towards radicals would be smaller. The kinetic constants that showed the smallest values were those associated to the iron redox cycle, k_1-k_3 and k_{2s}. Values of k_1 between 53 and 76 $M^{-1}s^{-1}$ and 0.002 $M^{-1}s^{-1}$ for k_3 (Eqs. 1 and 2) can be found in the literature (Pérez-Moya *et al.*, 2008). The value found for k_1 in the model was 350 $M^{-1}s^{-1}$, which is higher than the theoretical values. Nevertheless, the relationship between k_1 and k_3 is maintained ($k_1/k_3 \sim 10^3$). As for k_2, the value in the model is 3 $M^{-1}s^{-1}$, higher than k_3 as UV irradiance enhances the iron (III) reduction, and it is two orders of magnitude smaller than k_1, so it is also a consistent value. The value of k_{2s} is related with the saturation effect of UV irradiance. It corresponds to the value of irradiance which achieves half the maximum degradation rate. In this case, the value obtained was 7 $W\ m^{-2}$, which is consistent with the meaning of k_{2s} since the theoretical value would be the middle point between 0 and 15 $W\ m^{-2}$, which was where the irradiance saturation point was found.The values of parameters shown in Table 5 were used to validate the model, simulating the validation runs (which were not used to adjust the model) (Table 1). The results of the model fit are shown in Figure 3.

Each of the figures corresponds to one iron concentration, each one with a different irradiance value to widen the validation range. During the search of the parameters, the weight of the error for each variable (ACTM, TBZ, IMZ or H_2O_2) was not the same. The alpha value (see Methods Section), which is a weighting parameter, was highest for ACTM and H_2O_2. Certainly, when ACTM is completely removed, the other two pollutants are removed as well, so it is important to effectively simulate this variable. As for hydrogen peroxide, the successful prediction of its consumption is important for the process as it affect the process costs (Sánchez Pérez *et al.*, 2013b). Consequently, the parameter search was specially aimed at successfully modelling the two variables.

The model predicted remarkably well the hydrogen peroxide consumption in all the validation conditions (Figure 3). And ACTM degradation profiles could also be properly predicted for 5 and 20 $mg\ l^{-1}$ of iron (in Figure 3b and 3c). However, the predicted profile for 1 $mg\ l^{-1}$ Fe resulted in a slower degradation than the experimental values. This happened for IMZ and TBZ, although to a lesser extent, since the time for total removal could at least be predicted for these compounds. Their simulated profiles for higher iron concentrations were adequate.

The deviation in the prediction of ACTM degradation with 1 $mg\ l^{-1}$ Fe could be related to different factors. The most likely is that with only 1 $mg\ l^{-1}$ Fe, hydroxyl radical generation rate is strongly limited by the low amount of catalyst and more reaction mechanisms could take place, which were not considered in the simplified model, such as the reactions with transformation products. In any case, 1 $mg\ l^{-1}$ Fe would not be realistic for practical applications and it would be imperative to work with higher iron concentrations more suitable for process simulation.

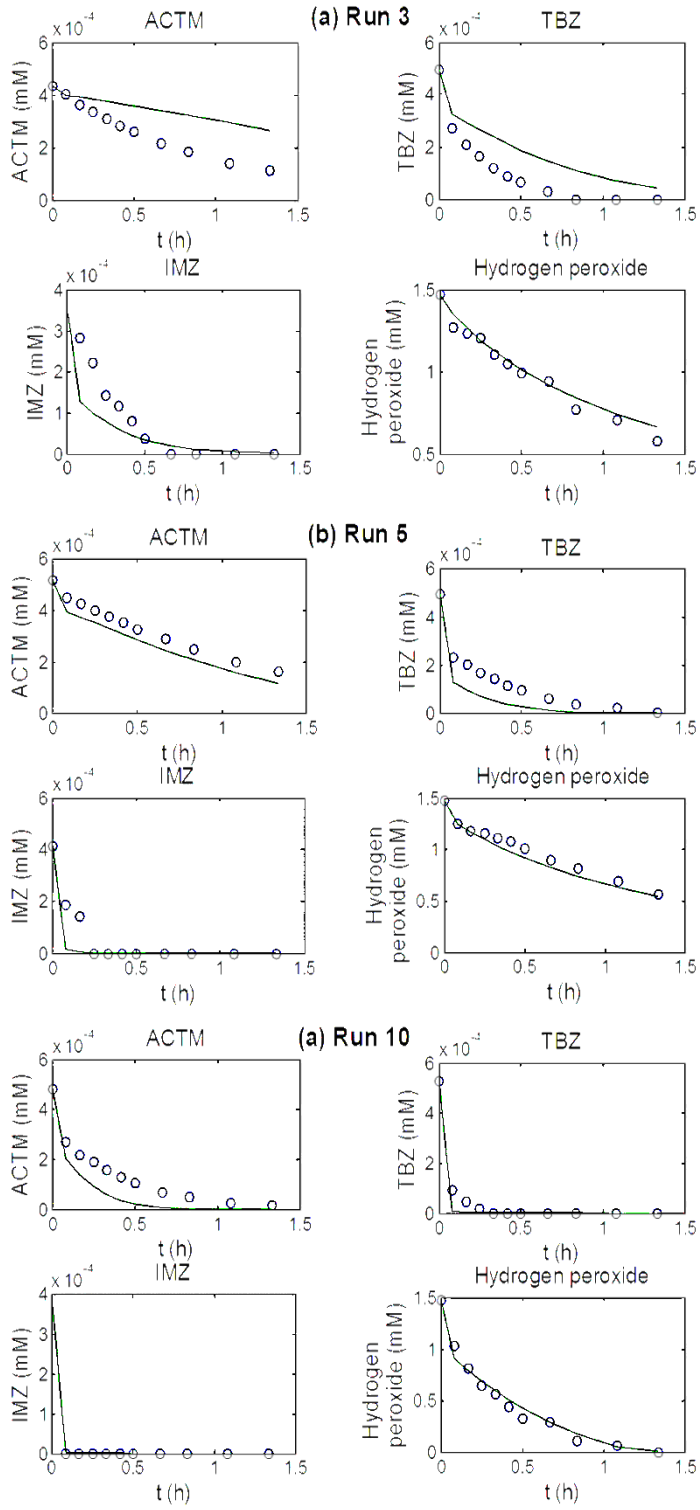

Figure 3. Experimental (dots) and predicted (lines) profiles for ACTM, TBZ and IMZ oxidation and hydrogen peroxide consumption for the model validation (runs 3, 5 and 10)

4. Conclusions

In this work we present a simplified kinetic model to simulate the solar photo-Fenton process applied to wastewater treatment plant secondary effluent to remove micropollutants in a wide range of iron concentration and irradiance. The model can be used to successfully predict micropollutant degradation

in tubular solar photoreactors during the whole year with iron concentrations between 5 and 20 mg l^{-1} Fe, which is a common interval in this process. This model can also be taken as the first step to optimize micropollutant degradation and hydrogen peroxide dosage, permitting automatisation.

ACKNOWLEDGEMENTS

This research was supported by the Ministerio de Economía y Competitividad (CTQ2010-20740-C03-01/PPQ), the European Regional Development Fund (ERDF). Irene Carra would like to acknowledge the Ministerio de Educación, Cultura y Deporte for her FPU scholarship (AP2010-3218).

References

Al Aukidy M., Verlicchi P., Jelic A., Petrovic M. and Barceló D. (2012), Monitoring release of pharmaceutical compounds: Occurrence and environmental risk assessment of two WWTP effluents and their receiving bodies in the Po Valley, Italy, *Science of the Total Environment*, **438**, 15-25.

Bernabeu A., Vercher R.F., Santos-Juanes L., Simón P.J., Lardín C., Martínez M.A., Vicente J.A., González R., Llosá C., Arques A. and Amat A.M., (2011) Solar photocatalysis as a tertiary treatment to remove emerging pollutants from wastewater treatment plant effluents, *Catalysis Today*, **161**, 235-240.

Blanco J., Torrades F., Morón M., Brouta-Agnésa M. and García-Montaño J. (2013), Photo-Fenton and sequencing batch reactor coupled to photo-Fenton processes for textile wastewater reclamation: Feasibility of reuse in dyeing processes, *Chemichal Engineering Journal,* In Press, http://dx.doi.org/10.1016/j.cej.2013.10.101.

Bueno M. J. M., Gomez M. J., Herrera S., Hernando M.D., Agüera A. and Fernández-Alba A. R. (2012), Occurrence and persistence of organic emerging contaminants and priority pollutants in five sewage treatment plants of Spain: Two years pilot survey monitoring, *Environmental Pollution* ,**164**, 267-273.

Cabrera Reina A., Santos-Juanes Jordá L., García Sánchez J. L., Casas López J. L. and Sánchez Pérez J. A. (2012), Modelling photo-Fenton process for organic matter mineralization, hydrogen peroxide consumption and dissolved oxygen evolution, *Applied Catalysis B: Environmental*, **119– 120**, 132-138.

De la Cruz N., Giménez J., Esplugas S., Grandjean D., de Alencastro L. F. and Pulgarín C. (2012), Degradation of 32 emergent contaminants by UV and neutral photo-Fenton in domestic wastewater effluent previously treated by activated sludge, *Water Research*, **46**, 1947-5.

Gogate P.R. and Pandit A.B. (2004), A review of imperative technologies for wastewater treatment II: hybrid methods, *Advances in Environmental Research*, **8**, 553-597.

Hisaindee S., Meetani M.A. and Rauf M.A. (2013), Application of LC-MS to the analysis of advanced oxidation process (AOP) degradation of dye products and reaction mechanisms, *Trends in Analytical Chemistry*, **49**, 31-44.

Ikehata K. and El-Din M.G. (2006), Aqueous pesticide degradation by hydrogen peroxide/ultraviolet irradiation and Fenton-type advanced oxidation processes: a review, *Journal of Environmental Engineering and Science*, **5**, 81-135.

Karcin A. (2013), Degradation of chlorophenols and alkylphenol ethoxylates, two representative textile chemicals, in water by advanced oxidation processes: The state of the art on transformation products and toxicity, *Chemosphere*, In press doi: 10.1016/j.chemosphere.2013.10.034.

Klamerth N., Malato S., Agüera A. and Fernández-Alba A. (2013), Photo-Fenton and modified photo-Fenton at neutral pH for the treatment of emerging contaminants in wastewater treatment plant effluents: A comparison, *Water Research*, **47**, 833-40.

Kusic H., Koprivanac N., Horvat S., Bakija S. and Bozic A. L. (2009), Modeling dye degradation kinetic using dark- and photo-Fenton type processes, *Chemical Engineering Journa*l, **155**, 144-154.

Kusic H., Koprivanac N., Loncaric A. and Selanec I. (2006), Photo-assisted Fenton type processes for the degradation of phenol: a kinetic study, *Journal of Hazardous Materials*, **136,** 632–644.

Li Puma G., Khor J. N. and Brucato A. (2004), Modeling of an Annular Photocatalytic Reactor for Water Purification: Oxidation of Pesticides, *Environmental Science and Technology*, **38**, 3737–3745.

Malato Rodriguez S., Blanco Galvez J., Maldonado Rubio M.I., Fernandez Ibañez P., Alarcon Padilla D., Collares Pereira M., Farinha Mendes J. and Correia de Oliveira J. (2004), Engineering of solar photocatalytic collectors, *Solar Energy*, **77**, 513-524.

Malato S., Fernández-Ibáñez P., Maldonado M.I., Blanco J. and Gernjak W. (2009), Decontamination and disinfection of water by solar photocatalysis: Recent overview and trends, *Catalysis Today,* **147**, 1–59.

Michael I., Frontistis Z. and Fatta-Kassinos D. (2013), Removal of Pharmaceuticals from Environmentally Relevant Matrices by Advanced Oxidation Processes (AOPs), *Comprehensive Analytical Chemistry,* **62**, 345–407.

Mitroka S., Zimmeck S., Troya D. and Tanko J. M. (2010), How Solvent Modulates Hydroxyl Radical Reactivity in Hydrogen Atom Abstractions, *Journal of the American Chemical Society*, **132**, 2907-2913.

Nogueira R.F.P, Oliveira M.C. and Paterlini W.C. (2005), Simple and fast spectrophotometric determination of H2O2 in photo-Fenton reactions using metavanadate, *Talanta*, **66**, 86-91.

Ortelli D., Edder P. and Corvi C. (2005), Pesticide residues survey in citrus fruits, *Food Additives & Contaminants*, **22**, 423-428.

Ortiz de la Plata G., Alfano O. and Cassano A. (2010), Decomposition of 2-Chlorophenol Employing Goethite as Fenton Catalyst. I: Proposal of a Feasible, Combined Reaction Scheme of Heterogeneous and Homogeneous Reactions, *Applied Catalysis B: Environmental*, **95**,14–25.

Pérez-Moya M., Graells M., Buenestado P. and Mansilla H.D. (2008), A comparative study on the empirical modeling of photo-Fenton treatment process performance, *Applied Catalysis B: Environmental*, **84**, 313–323.

Sánchez Peréz J.A., Carra I., Sirtori C., Agüera A. and Esteban B. (2013a), Fate of thiabendazole through the treatment of a simulated agro-food industrial effluent by combined MBR/Fenton processes at μg/L scale, *Water Research*, In Press, http://dx.doi.org/10.1016/j.watres.2013.07.039.

Sánchez Pérez J.A., Román Sánchez I.M., Carra I., Cabrera Reina A., Casas López J.L. and Malato S. (2013b), Economic evaluation of a combined photo-Fenton/MBR process using pesticides as model pollutant. Factors affecting costs, *Journal of Hazardous Materials*, **244-245**, 195-203.

Zhang R., Vigneswaran S., Ngo H. and Nguyen H. (2007), A submerged membrane hybrid system coupled with magnetic ion exchange (MIEX®) and flocculation in wastewater treatment, *Desalination*, **216**, 325-33.